ELSEVIER

Microporous Materials 11 (1997) 171–183

MICROPOROUS
MATERIALS

Zr-exchanged and pillared beidellite: preparation and characterization by chemical analysis, XRD and Zr K EXAFS

J. Miehé-Brendlé [a,*], L. Khouchaf [b], J. Baron [a], R. Le Dred [a], M.-H. Tuilier [b]

[a] *Laboratoire de Matériaux Minéraux (URA CNRS 428), E.N.S.C.Mu., Université de Haute Alsace, 3 rue A. Werner, F-68093, Mulhouse, France*

[b] *Laboratoire de Physique et de Spectroscopie Electronique (URA CNRS 1435), F.S.T., Université de Haute Alsace, 4 rue des frères Lumière, F-68093, Mulhouse, France*

Received 30 January 1997; accepted 30 April 1997

Abstract

Zirconia-pillared clays (with synthetic beidellite as host material) were prepared by replacing the sodium interlayer cations by zirconium hydroxy polycations, and then heating to stabilize the structure. The pillaring solution was an aqueous zirconyl chloride solution. The process was first optimized in order to decrease the volume of solution and the reaction time. From the XRD results, the interlayer spacing was found to be near 9 Å in Zr-exchanged beidellite and slightly lower (7 Å) after calcination. The B.E.T. surface area equals 174 $m^2 g^{-1}$. In order to follow the pillaring process, an EXAFS study at the Zr K edge was carried out on crystalline zirconyl oxychloride, the pillaring solution, ion-exchanged and pillared beidellite. There is no difference between the nearest and next-nearest-neighbour environments of Zr in solid zirconyl oxychloride and the pillaring solution. Furthermore, it is found that the Zr environment of the zirconyl polycation is preserved in the pillaring process. Although the mean Zr–O and Zr–Zr distances are shortened from 2.21 and 3.59 Å, respectively, in exchanged beidellite to 2.17 and 3.38 Å, respectively, in the calcined material, the nearly square frame of the Zr_4 zirconyl units is also preserved after the calcination process. The results are consistent with the intercalation of zirconyl pillars made of isolated zirconyl polycations normal to the (001) planes of the beidellite layers. From the charge deduced from chemical analysis, one polycation cancels the charge of four unit cells of the beidellite. © 1997 Elsevier Science B.V.

Keywords: Pillared clays; Beidellite; EXAFS; Zirconium

1. Introduction

The main interest in clay pillaring is to generate tailor-made structures by controlling the size and population of pillars between the silicate layers. These materials have therefore potential applications as catalysts in hydrocarbon hydrocracking and a wide variety of proton catalyzed reactions. Pillared clays can be obtained from a wide range of both starting clay materials and pillaring agents. Among the various pillaring species, Zr is one of the few transition metals known to provide stable pillars [1–4] but, despite all the work already carried out in this field, the structure of the hydroxy-Zr compounds in the intercalated clay is not clearly established, and its transformation into

* Corresponding author.

PII S0927-6513(97)00041-2

ZrO_2 oxide particles has not really been determined. The intercalant solution is usually an aqueous solution prepared from zirconyl oxychloride $ZrOCl_2.8H_2O$. The structure is built up from $[Zr_4(OH)_8(H_2O)_{16}]^{8+}$ tetramers [5]. When dissolved in water, the solution becomes acidic owing to the hydrolysis of a few water molecules of the tetramers. Depending on the preparative method (concentration, pH, ageing temperature, ageing time…), the degree of polymerization of hydroxy zirconium species can be affected [6,7]. In freshly prepared solutions at room temperature, little polymerization is likely to take place, the species consist of the basic tetramer units or small oligomers [8,9], whereas heating or ageing the solution lead to hydrolytic polymerization of the zirconium ions in solution [4].

The resulting species are usually intercalated between the clay layers by ion exchange with the interlayer cations of the clay, forming Zr exchanged clays. On the basis of chemical analysis carried out on products prepared at room temperature, Yamanaka and Brindley [10] suggested that the tetrameric cation $[Zr_4(OH)_{14}(H_2O)_{10}]^{2+}$ is the pillaring species, whereas Ohtsuka et al. [11] concluded that the intercalated species is $[Zr_4(OH)_{11.2}(H_2O)_{12.7}Cl_{0.1}]^{4.7+}$

In the present paper, we first describe the zirconyl-exchange and pillaring procedure of synthetic beidellite. This starting material, with a formula per half a unit cell of $Na_x(Si_{4-x}Al_x)(Al_2\square)O_{10}(OH_{2-y},F_y),nH_2O$, is a dioctahedral smectite wherein the octahedral sheet contains two Al^{3+} cations and one vacancy ($\square$) and the tetrahedral Si cations are partly substituted by Al cations. The pillaring conditions (Zr to Na-beidellite molar ratio, ion-exchange time, preliminary water dispersion) were optimized in order to simplify the handling during pillaring. Indeed, the method which is usually employed, whatever the pillaring species, has many disadvantages for a use on an industrial scale. The process is generally carried out on a dilute clay suspension (from 0.5 to 20 wt.%) which is brought in contact with a dilute solution of the pillaring agent (from 0.1 to 1.5 M). This may involve handling of large volumes in relation to the amount of material to be pillared. To simplify the preparation from the operative point of view, beidellite is directly brought in contact with the pillaring solution, without a preliminary water dispersion, as previously done for pillaring with aluminium polycations [12–14]. The latter results are then compared with those obtained by using an aqueous suspension of beidellite (8.5 wt.%).

In the second part, an EXAFS study is discussed with the aim of comparing the local environment of zirconium in solid zirconyl oxychloride, in the pillaring solution, in ion-exchanged and pillared beidellite, in an attempt to follow the modification of the pillaring species after intercalation and calcination.

2. Experimental

2.1. Starting material

The host clay was a Na-beidellite synthesized in an acidic fluoride medium under hydrothermal conditions according to Huve et al. [15].

A hydrogel of molar composition $1SiO_2$: 0.36 Al_2O_3: 0.14 NaF: 0.1 HF: 48 H_2O was prepared. Hydrofluoric acid (Fluka, 40% water) was added to distilled water, then sodium fluoride (NaF, Prolabo 98%) was dissolved. After dissolution, the alumina (AlOOH, Vista Catapal B pseudoboehmite containing 31 wt.% water) and silica sources (Aerosil 130, Degussa) were added. This mixture was matured for 4 h at room temperature before being heated in a PTFE-lined stainless-steel autoclave at 220°C under autogenous pressure during 3 days. After crystallization, the autoclave was cooled to room temperature. The product was filtered, washed with distilled water and dried at 60°C for 12 h.

2.2. Preparative procedure

Fig. 1 presents the procedure used to optimize the intercalation of zirconium oxyhydroxy polycations into the interlayer spacing of beidellite. Details for each step are given next.

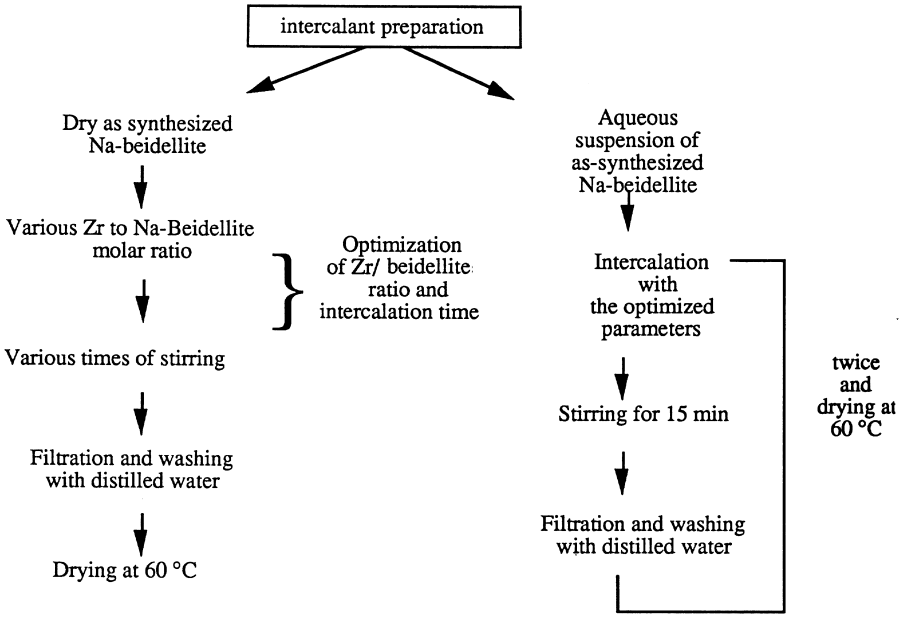

Fig. 1. Steps of the intercalation process.

2.2.1. Preparation of the intercalant

A 0.1 M zirconyl oxychloride aqueous solution was prepared from zirconyl oxychloride ($ZrOCl_2$, $8H_2O$, Fluka, 98%) just before use to avoid ageing and polymerization.

2.2.2. Intercalation

2.2.2.1. Zr to Na-beidellite molar ratio. 0.8 g of dried as synthesized Na-beidellite was added to different volumes (2–57 ml) of the 0.1 M Zr solution, to yield a Zr to Na-beidellite molar ratio (Zr/Na-beidellite) between 0.1 and 2.9. The mixtures were stirred for 5 min at room temperature, filtered and washed free of chloride ions with distilled water before being dried at 60°C.

2.2.2.2. Kinetic study. 0.8 g of dried Na-beidellite was fully dispersed in 19 ml of the intercalant solution (Zr/Na-beidellite = 0.95). After stirring for various times (5, 15, 30, 45 and 60 min), the exchanged beidellite was separated by filtration, washed and dried at 60°C.

2.2.2.3. Influence of the preliminary water dispersion and the number of ion-exchanges. In order to determine whether the preliminary water dispersion of dried Na-beidellite is necessary, 0.8 g of dried Na-beidellite was fully dispersed in 9.4 ml water for 30 min before addition of 19 ml of the 0.1 M Zr solution (Zr/Na-beidellite = 0.95). The concentration after dilution was 0.06 M. After stirring for 15 min, the exchanged beidellite was filtered and washed as previously described. Part of this sample was dried and the other part was directly redispersed in a 0.06 M Zr solution. After 15 min of stirring, the solid sample was filtered, washed and redispersed in a 0.06 M Zr solution and stirred for 15 min. This last treatment was followed by washing and air drying at 60°C.

2.2.3. Calcination

The samples were calcined at 500°C with a heating rate of 50 $C^\circ\,h^{-1}$. Once the calcination temperature was reached, the sample was kept at this temperature for 4 h before being slowly cooled at a rate of 50 $C^\circ\,h^{-1}$.

2.3. Characterization

The starting material was first examined by scanning electronic microscopy (SEM) on a Philips

XL30 microscope in order to determine its morphology. The X-ray powder diffraction (XRD) patterns were recorded on a Philips PW1800 automatic powder diffractometer employing CuKα radiation and with automatic divergence slits. Information about the phases present and the d_{001} spacing which is considered as one of the most characteristic parameters of intercalated and pillared clays was obtained with the APD 1700 software.

The ^{29}Si, ^{27}Al and ^{19}F magic angle spinning (MAS) nuclear magnetic resonance (NMR) spectra of the starting material were recorded on a Bruker MSL 300 spectrometer. The chemical shift standards used were $Si(CH_3)_4$, $Al(H_2O)_6^{3+}$ and $CFCl_3$, respectively. The spinning rate was 4 kHz for ^{29}Si and ^{27}Al and 8 kHz for ^{19}F. ^{29}Si MAS NMR provides information on the Si to Al ratio in the tetrahedral layer and consequently on the layer charge, whereas ^{27}Al MAS NMR indicates the localization of Al in the structure and ^{19}F MAS NMR confirms the substitution of fluoride ions for hydroxyl groups, and shows their environment.

Elemental analysis of Na-beidellite and Zr-exchanged and pillared beidellite was performed by the Service Central d'Analyse of the Centre National de la Recherche Scientifique (CNRS).

The thermogravimetric curves were obtained on a Mettler apparatus in an argon atmosphere with a heating rate of 4 C° min^{-1}.

The BET surface area measurements were carried out at the Institut Français du Pétrole (IFP) on a ϕ_{sorb} apparatus. The specific surface area was estimated by the BET method.

The X-ray absorption experiments were performed at the Laboratoire pour l'Utilisation du Rayonnement Electromagnétique (LURE, Orsay, France) on the XAS2 beam line of the DCI storage ring. The X-rays were monochromatized by a Si(311) two-crystal spectrometer. The X-ray absorption spectra were recorded at the Zr–K edge in transmission mode, at room temperature (RT) and 16 K, from three samples, $ZrOCl_2$, $8H_2O$ (powder), Zr-exchanged (sample EB) and pillared beidellite (sample PB). Moreover, the EXAFS data were obtained at RT from a 0.1 M $ZrOCl_2$ aqueous solution using an absorption cell which maintained liquid layers at 0.2–1 mm thickness between two kapton windows.

3. Results and discussion

3.1. Na-beidellite

The product was obtained with a yield as high as 95%. The SEM micrograph (Fig. 2) shows small aggregates of platelets similar to gypsum flower. This morphology, which prevents a preferential orientation of the sample, was also mentioned for beidellite synthesized in a basic medium [16]. The product is highly crystalline and virtually pure as shown by XRD (Fig. 3). The data for beidellite from Black Jack Mines [17] were used for indexing the *hk* bands. The spectrum exhibits the characteristic *hk* bands at 4.44 Å (02,11), 2.56 Å (13,20), and 1.487 Å (06,33). The latter reflection indicates the dioctahedral nature of the material. The (001) peak is located at 12.36 Å. Thus, the interlayer spacing is 2.76 Å, since the basal spacing (d_{001}) equals the thickness of the silicate layer (i.e. 9.60 Å for the beidellite) and the interlayer spacing. Some (001) reflexions are also present, with a (002) band at 6.20 Å and a (004) band at 3.09 Å. Assuming orthorhombic symmetry, the unit-cell parameters

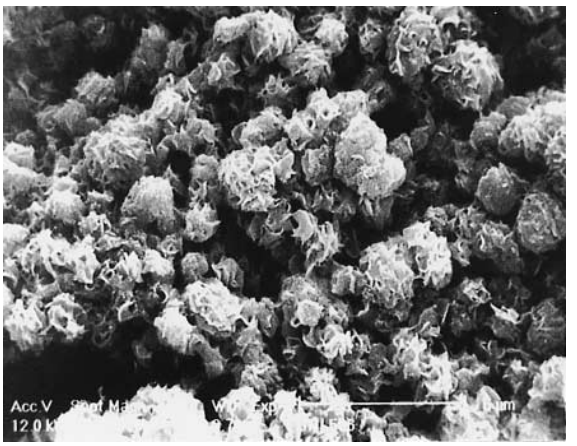

Fig. 2. SEM image of Na-beidellite synthezised in an acidic fluoride medium.

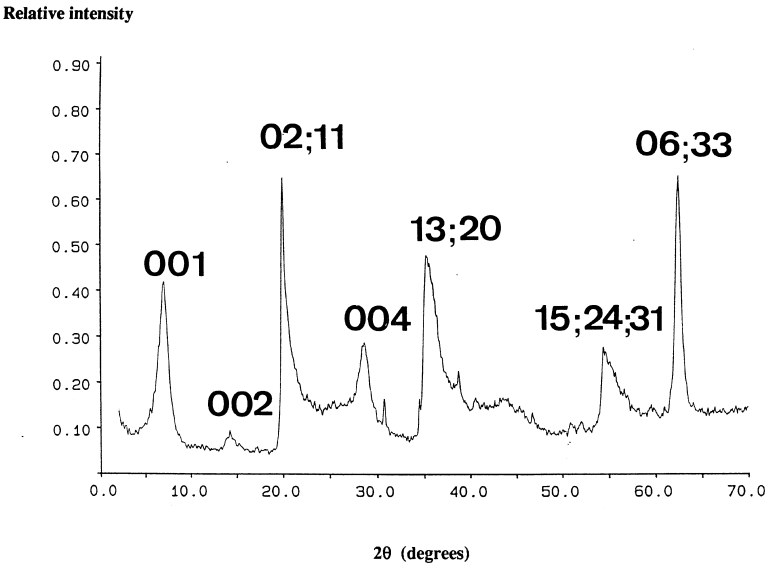

Fig. 3. XRD pattern of Na-beidellite synthezised in an acidic fluoride medium.

deduced from XRD are: $a = 5.15$ Å, $b = 8.92$ Å and $c = 12.36$ Å.

Evidence for one type of fluorine with a chemical shift, δ, of -132.5 ppm was provided by ^{19}F MAS NMR. This chemical shift is assigned to an $Al_2\square$ environment in the dioctahedral sheet [18], where $\square$ represents a vacancy. The presence of Al in the octahedral and tetrahedral layers was confirmed by ^{27}Al MAS NMR, the δ values are 1.5 and 66 ppm, respectively. The ^{29}Si MAS NMR spectrum shows signals corresponding to Si(nAl) environments where n represents the number of tetrahedral Al next-nearest neighbours to Si. The three signals at about -93, -88, and -82 ppm are respectively attributed to Si(0Al), Si(1Al) and Si(2Al) [19,20]. The Si/Al ratio in the tetrahedral layer can be determined from the relative contribution of the intensity of each Si(nAl) component by using Eq. (1) [21], where ISi(nAl) is the intensity of the NMR signal attributed to the Si(nAl) unit.

$$\left(\frac{\mathrm{Si}}{\mathrm{Al}}\right)_{\mathrm{tetra}} = \frac{\sum_{n=0}^{3} I\mathrm{Si}(n\mathrm{Al})}{\sum_{n=0}^{3} \frac{n}{3}\mathrm{Si}(n\mathrm{Al})} \qquad (1)$$

This formula is valid if it is assumed that no Al–O–Al linkage is present in the tetrahedral sheets, according to Loewenstein's rule. The knowledge of this ratio, which was found to be 6.9, allows us to calculate the tetrahedral layer charge x. This charge is given by Eq. (2) which is deduced from the chemical formula per half a unit cell:

$$x = \frac{4}{1 + \left(\frac{\mathrm{Si}}{\mathrm{Al}}\right)_{\mathrm{tetra}}} \qquad (2)$$

The experimental value 0.51 is in good agreement with the theoretical layer charge 0.50 and also in agreement with the ratio calculated from the chemical analysis. The Si and F contents determined by chemical analysis, and the weight loss determined by thermogravimetry lead to the following chemical formula per half a unit cell: $Na_{0.51}(Si_{3.49}Al_{0.51})(Al_2\square)O_{10}(OH_{1.58},F_{0.42})2H_2O$.

3.2. Zr-exchanged and pillared beidellite

The XRD d_{001} values (Table 1) for the samples obtained after one ion-exchange are plotted vs. the

Table 1
d_{001} (Å) as a function of the Zr/beidellite molar ratio

Zr to Na-beidellite molar ratio	0	0.09	0.19	0.48	0.67	0.95	1.92	2.87
Full width at half of the (001) reflexion	1.41	1.79	2.13	2.22	2.02	1.89	1.86	2.5
2θ	7.1	6.8	6.2	5.9	5.7	5.5	5.8	6.1
d_{001} (Å)	12.4	12.9	14.2	14.9	15.4	15.9	15.3	14.4

Zr to Na-beidellite molar ratio in Fig. 4. Up to a molar ratio of 0.7, there is a constant increase in the d_{001} value and a broadening of the (001) peak. This indicates, in particular, that even for a really short ion-exchange time (5 min), there is a replacement of part of the Na^+ cations by zirconium species. For a molar ratio of 0.95, the interlayer spacing is equal to 6.3 Å (experimental d_{001} value minus 9.6 Å which is the thickness of the sheet). This value is practically the same as that obtained by Ohtsuka et al. [11] after 3 h of ion-exchange and below the 9 Å usually mentioned for exchanged montmorillonite [10]. As already mentioned in the literature, we notice a decrease of the d_{001} values beyond a Zr to clay ratio of 0.95. Such a behaviour may be explained by a different arrangement of the species between the silicate layers. The Zr/Na-beidellite molar ratio equalling 0.95 was chosen for the following experiments.

The kinetic study performed with the Zr/beidellite molar ratio of 0.95 shows that whatever the stirring time, the d_{001} values are in the range 15.9–16.3 Å. Thus, it seems that the ion-exchange time is not a critical parameter for the intercalation process at these concentrations. This

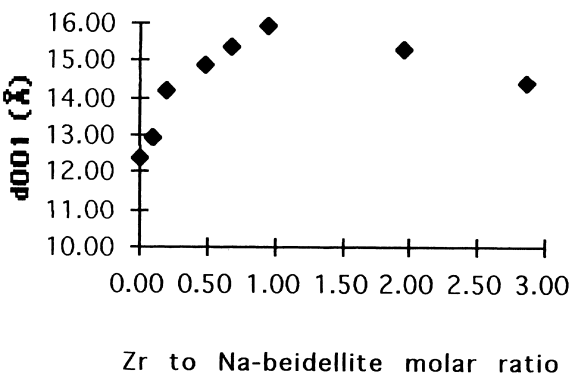

Fig. 4. d_{001} value as a function of Zr to Na-beidellite molar ratio.

result was also mentioned in a previous study of alumina $[Al_{13}O_4(0H)_{24}(H_2O)_{12}]^{7+}$ exchanged beidellite [12]. The molar ratio 0.95 and 15 min of ion-exchange time were chosen for further experiments.

It turns out that swelling of Na-beidellite by water dispersion is an important step. As a matter of fact, the addition of 19 ml of 0.1 M Zr solution to an aqueous suspension of Na-beidellite (1 g in 9.4 ml water) followed by 15 min of stirring leads indeed to a product having a d_{001} value equal to 17 Å. The first XRD reflection is sharp and symmetrical, indicating a regular ordering of the zirconium species (Fig. 5).

Moreover, two other treatments with a 0.06 M Zr solution without drying the beidellite led to a basal spacing of 18.2 Å and a very sharp first diffraction peak (Fig. 5).This corresponds to an interlayer spacing of 8.6 Å. Chemical analysis indicates that 0.09 mol Na ($n_{Na\ remaining}$) remain in exchanged beidellite and 0.43 mol Zr (n_{Zr}) are taken up after intercalation per half a unit cell. Since the layer charge equals 0.51 ($n_{Na\ initial}$), the degree of ion exchange equals 88.3%. This value is intermediate between that obtained by Ohtsuka et al. [11] after 24 h of ion exchange (77%) and that of Yamanaka and Brindley [10] (94%) after 1 h. The apparent charge per zirconium can also be calculated by the following formula if it is assumed that the layer charge remains constant during the ion exchange step:

$$y = \frac{(n_{Na\ initial} - n_{Na\ remaining})}{n_{Zr}}$$

This charge y is close to 1 within experimental error.

The specific surface area was equal to 174 $m^2\ g^{-1}$, which is about three times the surface area of the initial Na-beidellite (59 $m^2\ g^{-1}$).

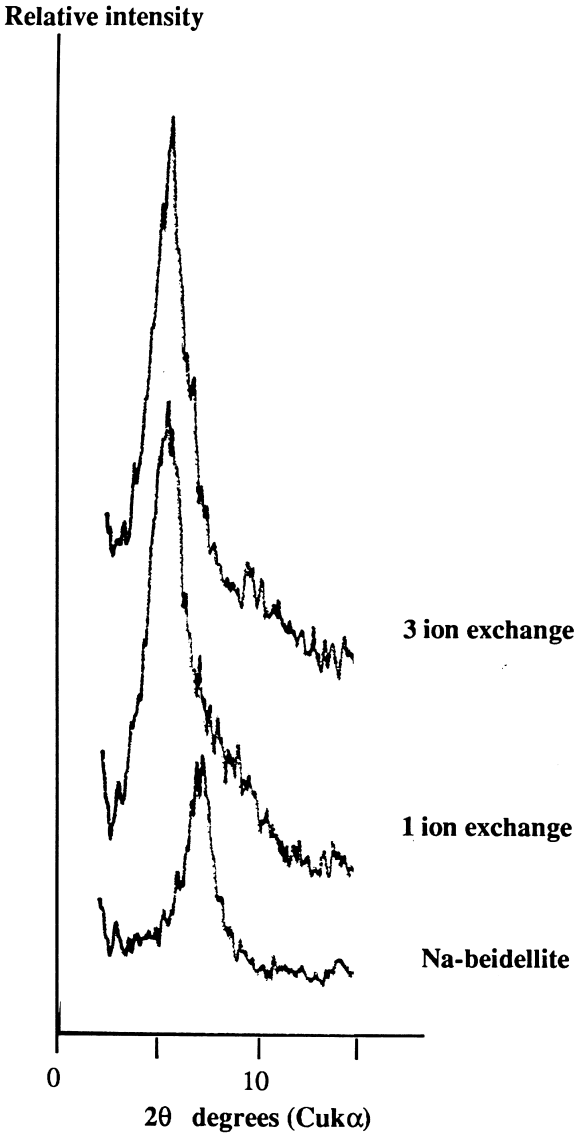

Fig. 5. (001) reflexion of Na-beidellite and Zr-exchanged beidellite after 1 and 3 ion exchange treatments.

Calcination at 500°C leads to a decrease of the basal spacing to 16.5 Å. Therefore, the interlayer spacing is found to be 6.9 Å. The contraction from 8.6 to 6.9 Å is mainly owing to the dehydratation and dehydroxylation of the Zr polycations during the calcination.

The process leading to the materials studied by EXAFS is summarized in Fig. 6.

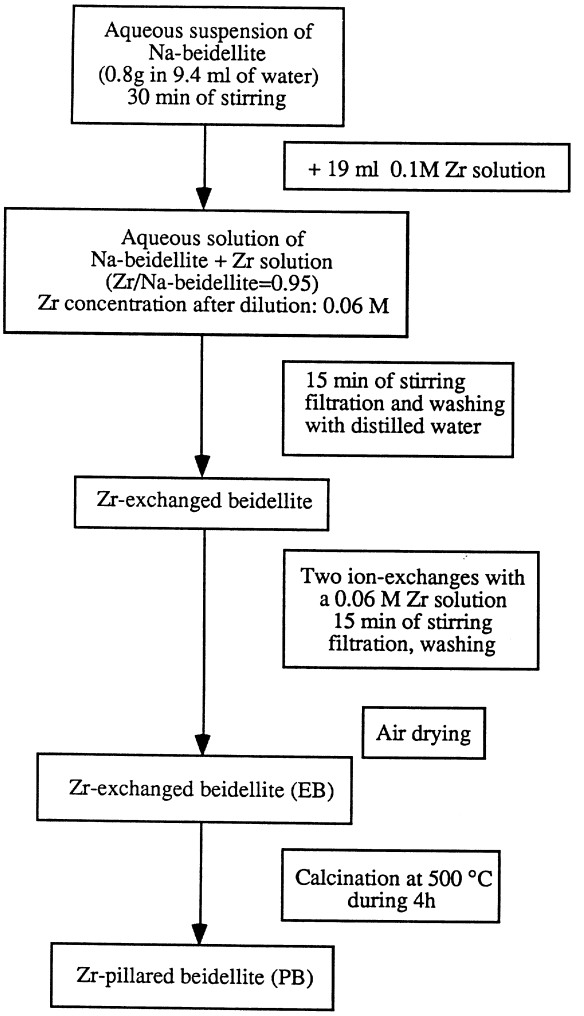

Fig. 6. Various steps of the process used to prepare the samples EB end PB.

3.3. EXAFS data reduction

The spectra were analysed using the software "EXAFS pour le Mac" [22]. After background substraction and conversion to k-space, the $\chi(k)$ EXAFS data were k^3 weighted and Fourier transformed between 3 and 15 $Å^{-1}$ (reference samples: $ZrOCl_2.8H_2O$ and 0.1 M aqueous solution) and 3 and 12 $Å^{-1}$ (beidellite samples) into the radial coordinate space (R-space) for a separation of different shells. EXAFS theory based on the single-scattering was used and the $\chi(k)$ EXAFS modula-

tion of the absorption coefficient is given by:

$$\chi(k) = -\sum_i N_i f_i(k) \sin[2kR_i + \phi_i(k)]$$

The summation extends over all neighbours' shells separated from the absorbing atom by a distance R_i. $\phi_i(k)$ is the total phase shift absorber–backscatterer pair and $f_i(k)$ is the backscattering amplitude including deviations from the average coordination radii estimated from the Debye–Waller parameter σ_i. N_i is the coordination number in each neighbour shell. Theoretical phase shifts and backscattering (BS) amplitudes generated by the *ab-initio* multiple scattering X-ray absorption code FEFF 6 [23] were used in the simulations of reference samples. The phase shifts $\phi_i(k)$ and BS amplitudes $f_i(k)$ for the the Zr–O pair were extracted from the analysis of the $ZrOCl_2 \cdot 8H_2O$ using the structural parameters of Ref. [5]. The uncertainty of the derived structural parameters was estimated from the variation of the parameter which gives twice the maximum residue.

3.4. EXAFS results and discussion

Fig. 7 shows the raw $k\chi(k)$ EXAFS data recorded at the Zr–K-edge from the pillaring precursor $ZrOCl_2 \cdot 8H_2O$ crystal (a) at 16 K, (b) at RT, (c) Zr pillaring solution at RT, (d) Zr-exchanged beidellite at 16 K and (e) calcined Zr-exchanged beidellite (16 K) after normalization to the Zr–K-edge, background removal and conversion to k-space.

3.4.1. $ZrOCl_2 \cdot 8H_2O$ and aqueous solution

The zirconyl oxychloride $ZrOCl_2 \cdot 8H_2O$ belongs to the space goup $P\bar{4}2_1c$.The unit cell parameters are 17.08 ± 0.02 Å and $c = 7.69 \pm 0.01$ Å [5]. The $ZrOCl_2 \cdot 8H_2O$ unit cell is drawn in Fig. 8. As previously described, four Zr cations are located at the corner of a slightly distorted square and linked along each edge of the square by two OH groups, one above and one below the plane of the square. Four water molecules are bonded to each zirconium atom and the arrangement of the eight oxygens around Zr^{4+} is a distorted antiprism. The distribution of the eight Zr–O bond lengths spreads over 0.28 Å with three range of distances,

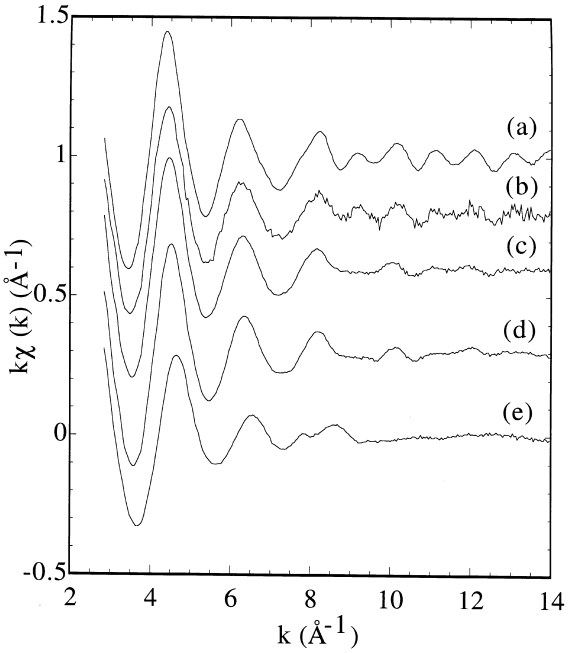

Fig. 7. $k\chi(k)$ EXAFS recorded at Zr–K-edge from (a) solid $ZrOCl_2 \cdot 8\ H_2O$ (16 K); (b) solid $ZrOCl_2 \cdot 8\ H_2O$ (RT); (c) $ZrOCl_2$ solution (RT); (d) Zr-exchanged beidellite (EB) (16 K); (e) pillared beidellite (PB) (16 K).

viz. 2.09–2.13 Å, 2.22–2.23 Å and 2.35–2.37 Å, respectively, and the average value of the nearest neighbour (NN) distance is 2.24 Å. The Zr cations have two Zr next-nearest neighbours (NNN) at 3.57 Å. The Fourier transforms (FT) between 3 and 15 $Å^{-1}$ of the k^3 weighted $\chi(k)$ data recorded from $ZrOCl_2 \cdot 8H_2O$ (crystal) and Zr pillaring solution are compared in Fig. 9. The curves exhibit two main peaks corresponding to oxygen and zirconium backscatterers at 1.8 and 3.2 Å, respectively. Their Fourier filtered contributions were simulated in single scattering formalism using BS amplitude and phase shifts generated by the ab initio multiple scattering X-ray absorption code FEFF 6 [23].

The structural parameters inferred from this preliminary study are summarized in Table 2. More details on the data analysis are given in Ref. [24]. As a main conclusion, there is no major difference between the zirconyl ion present in solid $ZrOCl_2 \cdot 8H_2O$ and in the Zr pillaring solution, as suggested by Hannane et al. on the basis of Raman

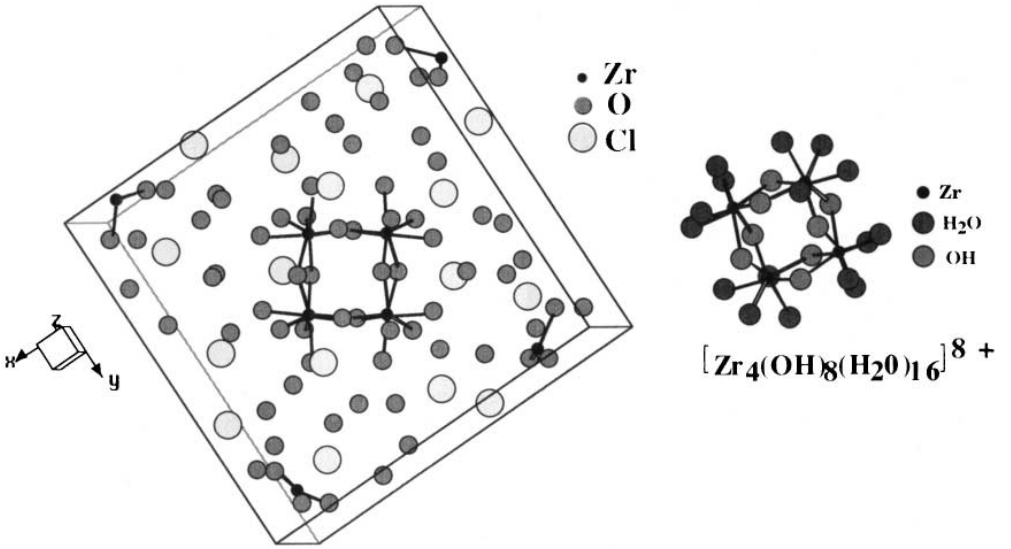

Fig. 8. Projection of one unit cell of $ZrOCl_2 \cdot 8H_2O$.

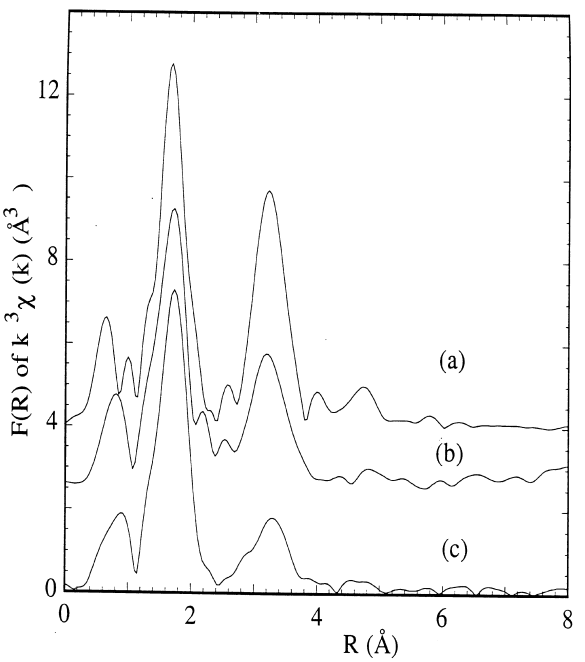

Fig. 9. Fourier transforms of $k^3\chi(k)$ data of: (a) solid $ZrOCl_2 \cdot 8\ H_2O$ (16 K); (b) solid $ZrOCl_2 \cdot 8\ H_2O$ (RT); (c) $ZrOCl_2$ solution (RT).

and ^{1}H-NMR studies [9]. Moreover, ageing during the measurements does not infer structural changes. At this stage, it can be assumed that the general formula of the polycation in solution is $[Zr_4(OH)_{16-n}(H_2O)_{8+n}]^{n+}$.

3.4.2. Zr-exchanged and pillared beidellite

The Fourier transforms of $k^3\chi(k)$ for Zr-exchanged (sample EB) and pillared (sample PB) beidellite are presented in Fig. 10. The two main peaks in the FT of EB correspond to oxygen NN and zirconium NNN. Their positions are quite the same as in the Zr pillaring solution (Figs. 11 and 12a). The simulations of their Fourier filtered contributions (Table 2) give 8 O neighbours at 2.21 Å and 1.3 Zr neighbours at 3.59 Å. These values are the same as in the Zr pillaring solution within the uncertainty of the EXAFS method. According to these results, the zirconium cations have the same environment in the interlayer spacing of beidellite as in the pillaring solution.

The FT (Fig. 10b) of pillared beidellite (PB) exhibits a clearly visible shift of the NN and NNN peaks towards the small coordination radii with respect to the exchanged radii (EB). The simulation of the NN filtered contribution (Fig. 11b) gives 6 O neighbours at 2.16 Å in PB instead of 8 O neighbours at 2.21 Å in EB. Let us consider the structure of monoclinic ZrO_2 [25], whose EXAFS has been extensively studied [26,27]. Seven Zr–O bonds ranging from 2.05 to 2.28 Å contribute to

Table 2
Structural parameters derived from Zr–K-EXAFS analysis

Samples	Zr–O (Å)	N_1	σ_1(Å)	Zr–Zr (Å)	N_2	σ_2 (Å)
$ZrOCl_2 \cdot 8H_2O$	2.22±0.02	8±1	0.10	3.57±0.02	1.9±0.5	0.03
0.1 M aqueous solution	2.22±0.01	7.9±0.8	0.10	3.58±0.04	1.2±0.8	0.07
EB	2.21±0.01	8±0.3	0.10	3.59±0.02	1.3±0.3	0.07
PB	2.16±0.02	6.1±1.4	0.11	3.38±0.02	1.9±0.6	0.11

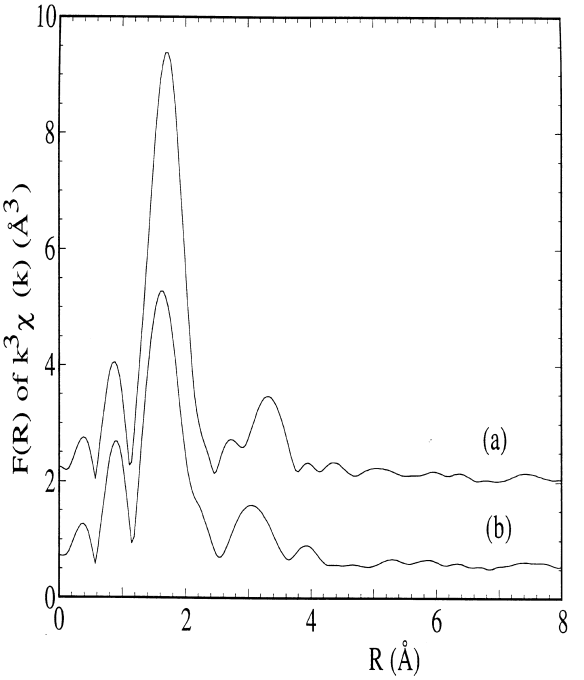

Fig. 10. Fourier transforms of $k^3\chi(k)$ data of: (a) Zr-exchanged beidellite; (b) pillared beidellite (PB).

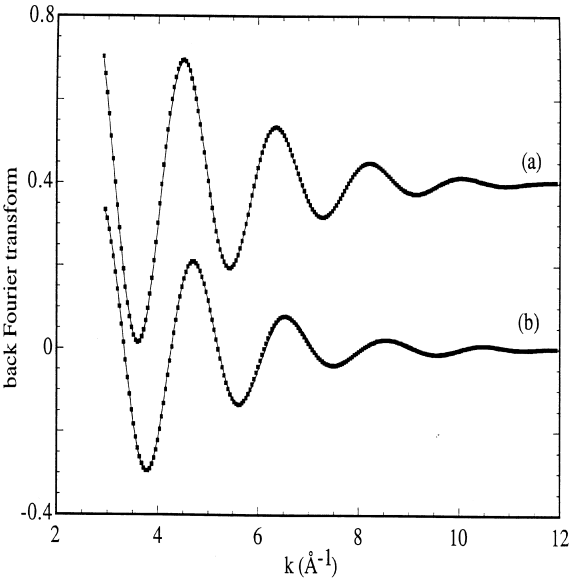

Fig. 11. Best fits (full line) performed on the Fourier-filtered NN shell contributions (dots) using the parameters reported in Table 2: (a) Zr-exchanged beidellite (EB); (b) pillared beidellite (PB).

the NN environment with an average value of 2.16 Å [26]. The mean Zr–O distance in PB is close to this value. The shortening of the bond length and decrease of the coordination number can be related to the dehydratation–dehydroxylation of the zirconyl cation during calcination. However, the removal of water molecules is associated with an increase of the σ DW parameter. The NN peak becomes asymmetric (Fig. 10b) with a tail on the great R-side. The information contained in the tail of the asymmetric distribution ($\sigma > 0.1$ Å) is not included in the result of the simulation which gives a mean distance of 2.16 Å for a Gaussian distribution of 6 neighbours around Zr. An explanation can be given by considering that one oxygen (or more) belonging to H_2O molecules is replaced by one oxygen (or more) bonded to Si or Al of the beidellite framework. According to this hypothesis, the zirconium coordination polyhedron becomes distorted after calcination, more than in monoclinic ZrO_2. One Zr–O bond (or more) is longer than the others and contributes only weakly to the NN distribution by an increase of σ.

The Zr–Zr distance derived from the simulation of the filtered contribution (Fig. 12b) of the NNN peak in PB is found to be 3.38 Å. When the NNN Zr-environment in PB and in monoclinic ZrO_2 are compared, it is found that the Zr cations have 12

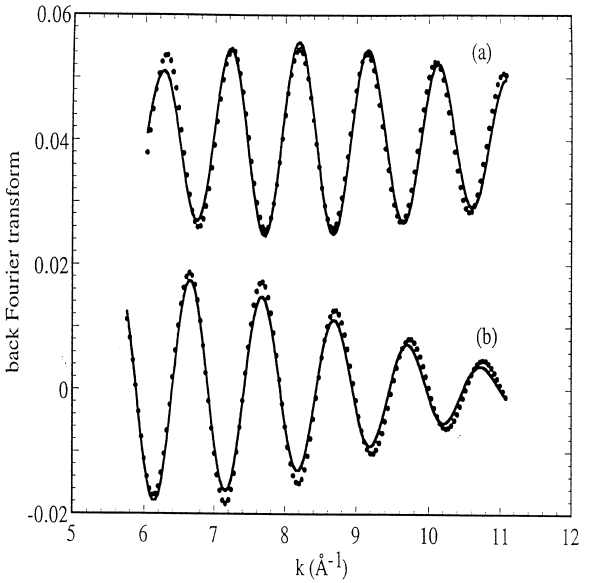

Fig. 12. Best fits (full line) performed on the Fourier-filtered NNN shell contributions (dots) using the parameters reported in Table 2: (a) Zr-exchanged beidellite (EB); (b) pillared beidellite (PB).

Zr neighbours, and the distribution spreads over 1.2 Å (from 3.34 to 4.54 Å) [26]. It was shown previously that the major contribution to the NNN distribution is owing to the first six Zr–Zr pairs with an average value of 3.43 Å and more recently to the first seven Zr–Zr pairs with an average value of 3.46 Å [27].The Zr–Zr distance in PB is smaller than in ZrO_2, showing that the pillar has not the structure of bulk ZrO_2. Furthermore, the coordination remains nearly the same as in EB. The frame of the zirconium oxide units formed in the interlayer spacing is not greatly modified after calcination (Fig. 14).

On the contrary, the calcination involves a dramatic decrease of the interlayer spacing of one order of magnitude greater than the decrease of the interatomic distances. Yamanaka and Brindley [10] proposed two models: either a flat lying complex or a single layer of complexes standing normal to the montmorillonite layer. In our case, the interlayer spacing (i.e. 8.6 Å) is too small before calcination to accommodate two layers of polycations even mismatched.

Furthermore, the former model disagrees with the EXAFS results since the Zr environment is the same in the pillaring solution as in EB, the dehydratation–dehydroxylation processes giving rise to a shortening of the interatomic distances in PB without strong changes in the framework of the zirconium units. Therefore, it can be assumed that the polycations are isolated, otherwise, the NNN environment will be modified. There is a good agreement between the latter model and the results of the EXAFS analysis as well as the interlayer spacing value.

Therefore, the Zr_4 frame of the zirconyl polycation is preserved during the exchange reaction and the calcination. Since this polycation has a general formula of $[Zr_4(OH)_{16-n}(H_2O)_{8+n}]^{n+}$ and the effective charge per Zr is close to 1, it is possible to determine the charge n^+ of this polycation. Indeed, there are four Zr atoms with an effective charge of 1 per atom in each polycation; consequently, n equals 4. One polycation cancels the charge of four unit cells of the beidellite. Such a polycation $[Zr_4(OH)_{12}(H_2O)_{12}]^{4+}$ carries four positive charges instead of two in the model of Ref. [10] and enables a symmetrical charge environment for each zirconium. Thus, each Zr cation will have the same behaviour during the preliminary dissolution of $ZrOCl_2$ (Fig. 13). The size of the $[Zr_4(OH)_{12}(H_2O)_{12}]^{4+}$ polycation is estimated to be about 9.1 Å in length and 5.5 Å in thickness, very close to the unit cell parameter ($a=5.1$ Å and $b=8.8$ Å) of sample EB. Such polycations appear very suitable for a vertical insertion in the interlayer spacing during the exchange reaction of the beidellite.

From these considerations, the model drawn in

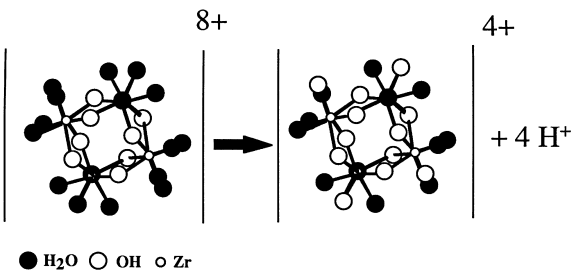

Fig. 13. Hydrolysis scheme leading to the $[Zr_4(OH)_{12}(H_2O)_{12}]^{4+}$ polycation during the intercalation in the interlayer space of beideillite.

Fig. 14 can be built for the structure of the exchanged beidellite. The circles represent the oxygen ions in one layer of the beidellite framework cut along the (001) plane. The rectangles figure the projection of the polycations, Zr_4 squares being vertical. Two of the four Zr cations are located either close to the middle of two adjacent hexagonal oxygen rings of the lower plane (model A in Fig. 14) or just above two oxygens anions of the surface belonging to the hexagonal cavity (model B in Fig. 14). Consequently, the Zr cations are probably bonded to some of the framework oxygen anions. The two others are in a symmetrical position of the upper plane which is not represented. The spacing of these units along the (001) plane is a function of the charge of the polycation and the beidellite lattice.

4. Conclusion

The comparative EXAFS study at the Zr–K-edge of the pillaring solution and Zr-exchanged beidellite reveals that the local order is the same in the solution and in the intercalated species. The atomic structure of the zirconyl polycation is preserved in the pillaring process described here. Furthermore, in spite of the decrease of the mean NN and NNN distances from 2.21 and 3.59 Å, respectively, in exchanged beidellite to 2.17 and 3.38 Å after calcination, the nearly square frame of the Zr_4 zirconyl units is preserved in calcined beidellite.

The value of 7 Å found for the spacing in the latter material is consistent with the model of zirconyl units which are normal to the (001) planes

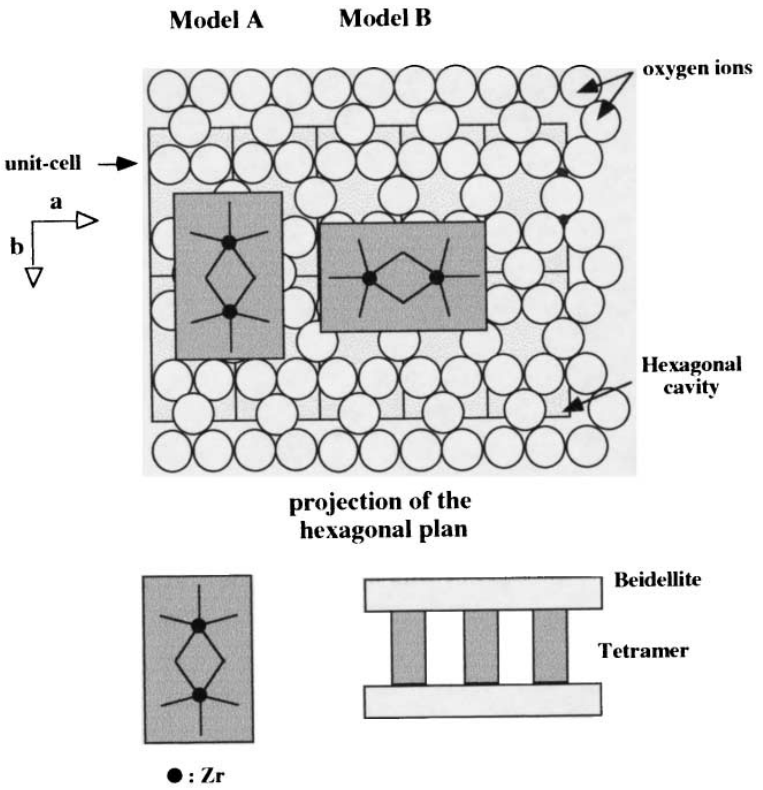

Fig. 14. Model showing the possible orientation of the $[Zr_4(OH)_{12}(H_2O)_{12}]^{4+}$ polycation in the interlayer space of beidellite. The hollow circles represent the oxygen ions in one layer of the beidellite framework cut along the (001) plane. The open rectangles indicate beidellite unit cells. The filled rectangles indicate the polycations with vertical Zr_4 squares. (A) and (B) are two possible sites for the latter.

of beidellite. The charge of the polycation is found to be close to 4 and consistent with a density of one zirconyl per four unit cells of the beidellite. The hypothesis of double layers proposed previously [10] should involve strong distortions of the Zr NNN during the calcination process and is inconsistent with our EXAFS results. The ideal position of the vertical pillars should be in such a way that the Zr cations share one or more bonds with the oxygen anions belonging to the hexagonal cavities of the beidellite. A study at the Si-K-edge is underway to gain some information on these bonds.

References

[1] K. Suzuki, M. Horio, H. Masuda, T. Mori, Bull. Chem. Soc. Jpn. 64 (1991) 732.
[2] R. Burch, C.I. Warburton, J. Catal. 97 (1986) 503.
[3] M.L. Occelli, D.H. Finseth, J. Catal. 99 (1986) 316.
[4] G.J. J Bartley, Catal. Today 2 (1988) 233.
[5] A. Clearfield, P. Vaughan, Acta Crystallogr. 9 (1956) 555.
[6] G.M. Muha, P.A. Vaughan, J. Chem. Phys. 33 (1960) 194.
[7] A. Clearfield, Rev. Pure Appl. Chem. 14 (1964) 91.
[8] F. Bertin, J. Bouix, S. Hannane, C.R. Acad. Sci. Paris 304 (1987) 405.
[9] S. Hannane, F. Bertin, J. Bouix, Bull. Soc. Chim. Fr. 127 (1990) 43.
[10] S. Yamanaka, G.W. Brindley, Clays Clay Miner. 27 (1979) 119.
[11] K. Ohtsuka, Y. Hayashi, M. Suda, Chem. Mater. 5 (1993) 1823.
[12] E. Benazzi, J. Miehe, J. Baron, R. Le Dred, D. Saehr, Fr Patent 94 06662, 1994.
[13] E. Benazzi, J. Miehe, J. Baron, R. Le Dred, D. Saehr, Fr Patent 94 06663, 1994.
[14] J. Miehe, R. Le Dred, D. Saehr, J. Baron, in: M.L. Occelli, H. Kessler (Eds.), Synthesis of Porous Materials, Zeolites, Clays, and Nanostructures, Marcel Dekker, New-York, 1996, p. 491.
[15] L. Huve, R. Le Dred, J. Baron, D. Saehr, in: M.L Occelli, H. Robson (Eds.), Expanded Clays and Other Microporous Solids, Van Nostrand, New York, 1992, p. 207.
[16] K. Yamagisawa, T. Kusunose, K. Ioku, N. Yamasaki, P.B. Malla, S. Kormaneni, J. Mater. Sci. Lett. 15 (1995) 861.
[17] D.M.C. MacEwan, G. Brown (Eds.), The X-ray Identification and Crystal Structures of Clay Minerals, Mineralogical Society, London, 1961, p. 143.
[18] L. Huve, L. Delmotte, P. Martin, R. Le Dred, J. Baron, D. Saehr, Clays Clay Miner. 40 (1992) 186.
[19] J. Sanz, J.M. Serratosa, J. Am. Chem. Soc. 106 (1984) 4790.
[20] A.W. Weiss, S.P. Altaner, R.J. Kirkpatrick, Am. Miner. 72 (1987) 985.
[21] G. Engelhardt, D. Michel, in: J. Wiley (Ed.), High Resolution Solid State NMR of Silicates and Zeolites, 1987, p. 485.
[22] A. Michalovicz, *Logiciels pour la Chimie*, Société FranÇaise de Chimie, Paris, 1991, p. 102.
[23] J. Mustre de Leon, J.J. Rehr, S.I. Albers, R.C. Albers, Phys. Rev. B 44 (1991) 4146.
[24] J. Miehe-Brendlé, L. Khouchaf, J. Baron, M.-H. Tuilier, Proceedings of the XAFS 9 Conference, Grenoble, 26–30 August, 1996, in press.
[25] D.K. Smith, H.W. Newkirk, Acta Crystallogr. 18 (1965) 983.
[26] M.-H. Tuilier, J. Dexpert-Ghys, H. Dexpert, P. Lagarde, J. Solid State Chem. 69 (1987) 153.
[27] P. Li, I.-W. Chen, J.E. Penner Hahn, Phys. Rev. B 48 (1993) 10063.